Materials Research Bulletin 176 (2024) 112816

Contents lists available at ScienceDirect

Materials Research Bulletin

journal homepage: www.elsevier.com/locate/matresbu

Research Papers

4f-4f absorption strength of Eu^{3+} in $La_2Zr_3(MoO_4)_9$ compared to other Eu^{3+} activated luminescent materials

Julia Exeler *, Thomas Jüstel

FH Münster University of Applied Sciences, Stegerwaldstr. 39, D-48565 Steinfurt, Germany

ARTICLE INFO

Keywords:
Luminescence
Anorganic chemistry
Material science
Physics
Chemistry

ABSTRACT

This study deals with the optical and luminescent properties of a double molybdate containing rare earth elements, specifically focusing on $La_2Zr_3(MoO_4)_9:Eu^{3+}$ and comparing it with the widely used $Y_2O_3:Eu^{3+}$, (Y,Gd)$BO_3:Eu^{3+}$ and $YVO_4:Eu^{3+}$ as well as $Y_2O_2S:Eu^{3+}$ and $Y(P,V)O_4:Eu^{3+}$ phosphors. It utilizes Kubelka Munk Theory to estimate the absorption strengths of these materials. Higher absorption coefficients indicate greater efficiency in absorbing light, leading to more intense and brighter luminescence. This investigation aims to assess $La_2Zr_3(MoO_4)_9:Eu^{3+}$ as a promising luminescent material for optoelectronics and solid state lighting by comparing its absorbance properties.

1. Introduction

Double molybdates containing rare earth elements are known for their microwave dielectric properties and low sintering temperatures [1]. Their optical and luminescent properties are promising for optical purposes and for the use in laser physics. [2] Compounds according to $R_2Zr_3(MoO_4)_9$ (R = La – Gd) exhibit a trigonal phase with space group of R-3c [3–8]. $La_2Zr_3(MoO_4)_9$ mostly sintered in the rather low temperature range of 700 - 800 °C, possesses excellent microwave dielectric properties and can also serve as a red-emitting phosphor upon activation by Eu^{3+} or it shows blue-purple luminescence if activated with Dy^{3+} and/or Eu^{3+}. [3,9,10] Other well-known red-emitting phosphors are $Y_2O_3:Eu^{3+}$, (Y,Gd)BO_3:Eu, YVO_4:Eu, $Y_2O_2S:Eu^{3+}$ and $Y(P,V)O_4:Eu^{3+}$ which produces intense red emission under UV excitation [11–13].

Y_2O_3 crystallizes in the cubic crystal system with the space group Ia-3 (#206) and is a widely used material. [14] Its luminescent properties make it a valuable phosphor for various applications such as plasma display panels, fluorescent lamps, field emission displays, and cathode-ray tubes. [15–20], while (Y,Gd)BO_3:Eu, and YVO_4:Eu were also considered as alternative emitter.

The Kubelka-Munk theory has been widely studied and applied in various technical fields for the calculation of absorption strength. This theory assumes that light is isotropically scattered within the material, and it models the reflected spectrum of a colored body based on material-dependent scattering and absorption functions. [21] The theory has been used to estimate absorption and scattering coefficients, one-dimensional light intensity distribution, and light penetration depth in the spectral range of 300–850 nm. [22] Additionally, simulations of the spectral dependence of Kubelka-Munk coefficients of absorption and scattering have shown good agreement with experimental results. [23] It has also been compared with other calculation methods, leading to empirical expressions for the scattering and absorption coefficients, which provide nearly the same results as exact theories. [24] Furthermore, the theory has been widely used to obtain optical properties from measured reflectance spectra in diffusive and non-diffusive regimes. [25] In the field of optics, the Kubelka–Munk formalism has been used as a parametrization method to extract scattering and absorption parameters for strongly absorbing, multiple-scattering systems in the resonant regime. [26] Upon the use of the reflectance data of different media and scattering coefficients which can be estimated from the particle size of the powder, the absorption of materials can be calculated in a semi-quantitative way under the assumption that the medium is homogeneous, isotropic, and infinite in extent. [27,28]

The physical properties, such as density and refraction index of the host medium play a crucial role in determining how effectively europium ions can absorb the incident light and subsequently luminesce. [29–31] If a specific luminescent material containing europium has a higher calculated absorption coefficient (A) than another material, it could be an indication that the former is more efficient at absorbing light in the relevant wavelength range for exciting europium ions. While a higher absorption coefficient does generally indicate more efficient absorption of incident light or radiation, it doesn't guarantee brighter

* Corresponding author.
E-mail address: julia.exeler@fh-muenster.de (J. Exeler).

https://doi.org/10.1016/j.materresbull.2024.112816
Received 11 January 2024; Received in revised form 26 March 2024; Accepted 31 March 2024
Available online 1 April 2024

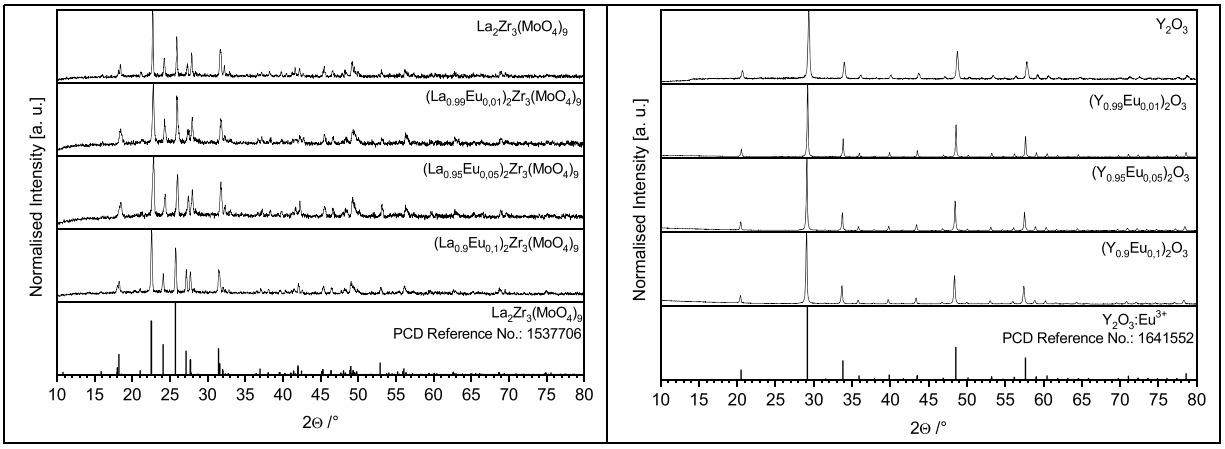

Fig. 1. XRD patterns of the synthesized $(La_{1-x}Eu_x)_2Zr_3(MoO_4)_9$ and $(Y_{1-x}Eu_x)_2O_3$ with $x = 0$, 0.01, 0.05, 0.1 and reference XRD patterns of $La_2Zr_3(MoO_4)_9$ and Y_2O_3:Eu^{3+}.

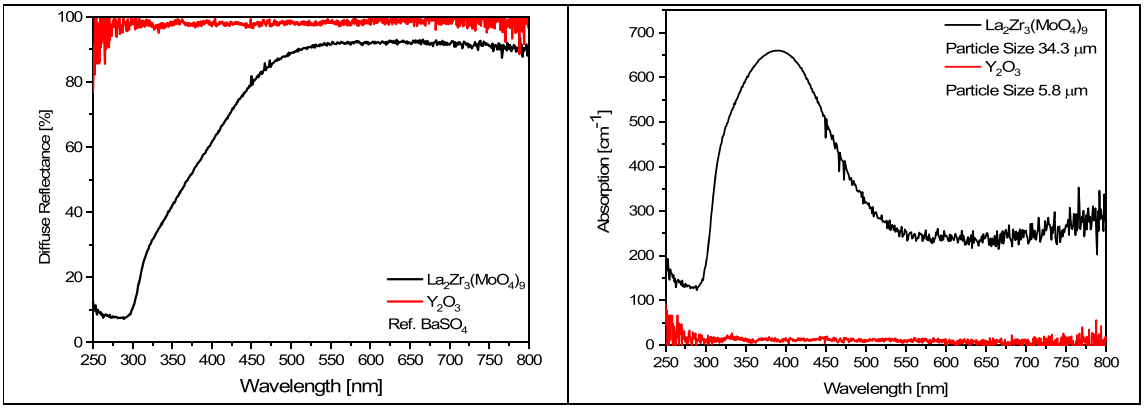

Fig. 2. a) Reflection spectra of $La_2Zr_3(MoO_4)_9$ and Y_2O_3 b) Qualitative absorption spectra of $La_2Zr_3(MoO_4)_9$ and Y_2O_3.

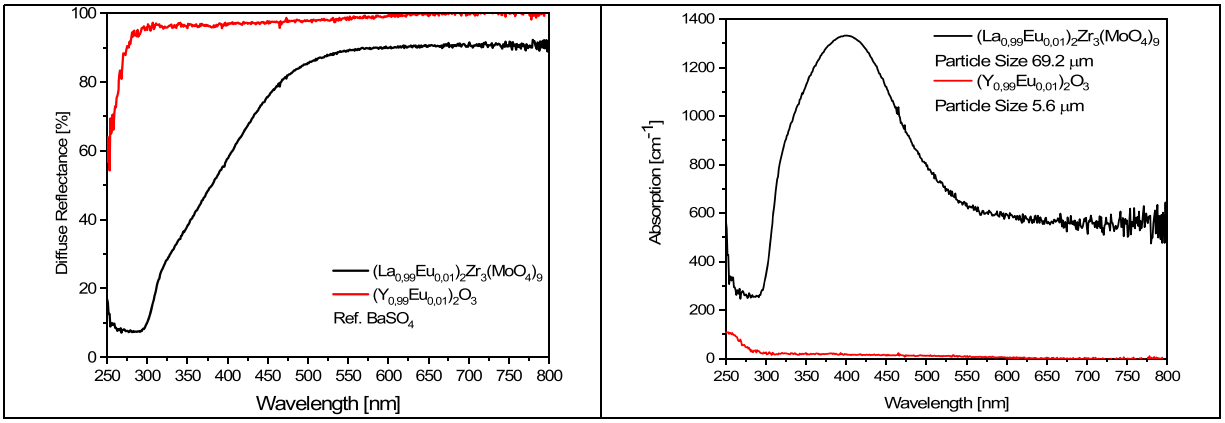

Fig. 3. a) Reflection spectra of $(La_{0,99}Eu_{0,01})_2Zr_3(MoO_4)_9$ and $(Y_{0,99}Eu_{0,01})_2O_3$ b) Absorption spectra of $(La_{0,99}Eu_{0,01})_2Zr_3(MoO_4)_9$ and $(Y_{0,99}Eu_{0,01})_2O_3$.

luminescence. Luminescence intensity also depends on factors such as the quantum yield of the luminescent process and thus with all non-radiative pathways that will compete with luminescence. Therefore, while higher absorption can be advantageous, it's not the sole determinant of luminescence brightness. In practical applications of europium-based luminescent materials, higher absorption can be advantageous, as it can lead to higher luminescent efficiency and brighter emission [32,33]. In this work, $La_2Zr_3(MoO_4)_9$:Eu^{3+} is investigated for absorbance and luminescent properties and compared with the well-known phosphor Y_2O_3:Eu^{3+} and other commercial used Eu^{3+}phosphors as it is a promising material for further use in opto-electronics and lightning technologies.

2. Experimental section

Powder samples of $La_2Zr_3(MoO_4)_9$ with 0%,1%, 5%, and 10% Eu^{3+} were prepared by conventional solid-state reactions. The starting materials were stochiometric amounts of high purity La_2O_3 (99.99 %,

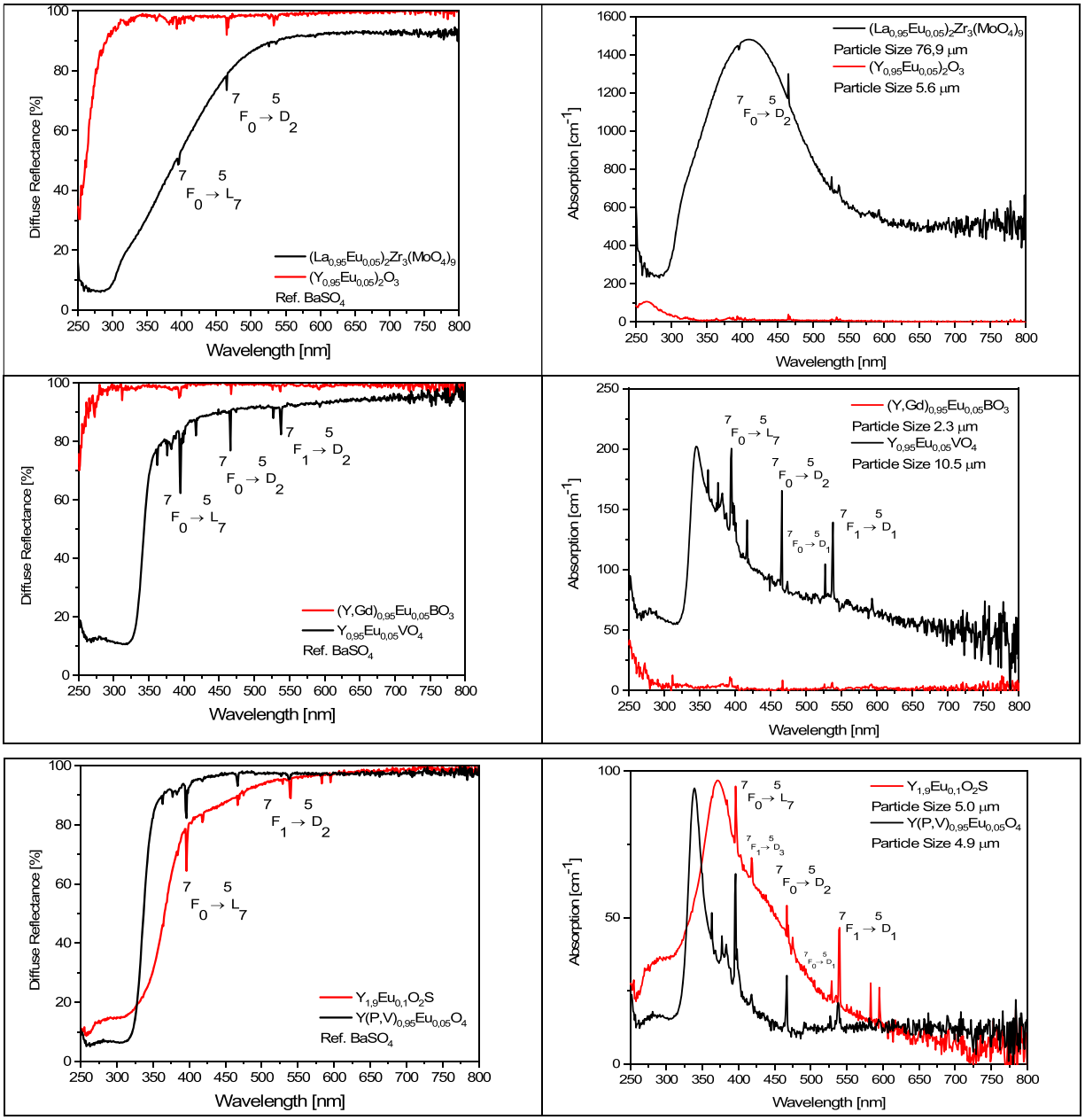

Fig. 4. a) Reflection spectra of $(La_{0,95}Eu_{0,05})_2Zr_3(MoO_4)_9$ and $(Y_{0,95}Eu_{0,05})_2O_3$ b) Absorption spectra of $(La_{0,95}Eu_{0,05})_2Zr_3(MoO_4)_9$ and $(Y_{0,95}Eu_{0,05})_2O_3$ c) Reflection spectra of $(Y,Gd)_{0,95}Eu_{0,05}BO_3$ and $Y_{0,95}Eu_{0,05}VO_4$ d) Absorption spectra of $(Y,Gd)_{0,95}Eu_{0,05}BO_3$ and $Y_{0,95}Eu_{0,05}VO_4$ e) Reflection spectra of $Y_{1,9}Eu_{0,1}O_2S$ and $Y(P,V)_{0,95}Eu_{0,05}O_4$ f) Absorption spectra of $Y_{1,9}Eu_{0,1}O_2S$ and $Y(P,V)_{0,95}Eu_{0,05}O_4$.

Treibacher Industrie AG), ZrO_2 (pro analysi, Aldrich), MoO_4 (99.9 %, Alfa Aesar) and Eu_2O_3 (99.99 %, Treibacher Industrie AG). The mixture was thoroughly mixed in an agate mortar with added acetone as grinding medium. After drying, the mixtures were transferred to alumina crucibles and calcinated in air at 1173 K for 4 h.

Y_2O_3 samples with equivalent parts of Eu^{3+} were prepared by precipitation. The starting materials consisting of Y_2O_3 (99.9 %, Treibacher Industrie AG) and Eu_2O_3 (99.99 %, Treibacher Industrie AG) were completely dissolved in HNO_3 and precipitated by the addition of oxalic acid. After drying, the mixtures were transferred to alumina crucibles and calcinated in air at 1600 K for 4 h.

X-Ray diffraction (XRD) analysis using a RIGAKU MiniFlex II as well as reflection spectra using Edinburgh Instruments FLS 920 spectrometer against $BaSO_4$ as background reference and ultrasonic particle size measurements (HORIBA Partica Laser Scattering Particle Size Distribution Analyzer LA-950V2) were performed. The data of measured reflection spectra and particles sizes were used to calculate absorption spectra by using Kubelka-Munk theory.

3. Results and discussion

As mentioned before, the structures of $La_2Zr_3(MoO_4)_9$ and Y_2O_3 were published and discussed by Liu et al. and Yong-Nian et al. [3,14] There are entries in the Pearson's Crystal Data Crystal Structure database for $La_2Zr_3(MoO_4)_9$, $Eu_2Zr_3(MoO_4)_9$ as well as Y_2O_3:Eu^{3+}. In previews works by Baur and Jüstel in 2015 a new red-emitting phosphor $La_2Zr_3(MoO_4)_9$:Eu^{3+} and the influence of host absorption on its luminescence efficiency was published and discussed [9]. However in the aforementioned publication there was no investigation of its absorbance and no comparison with well-known red-emitting phosphors to investigate whether $La_2Zr_3(MoO_4)_9$:Eu^{3+} could compete with standard materials like Y_2O_3:Eu^{3+}. In this work, powder samples of $(La_{1-x}Eu_x)_2Zr_3(MoO_4)_9$ and $(Y_{1-x}Eu_x)_2O_3$

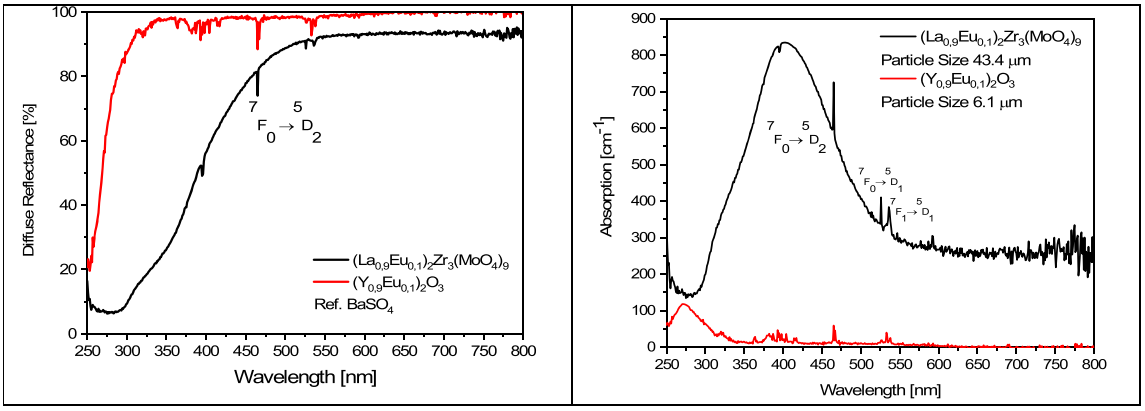

Fig. 5. a) Reflection spectra of $(La_{0,9}Eu_{0,1})_2Zr_3(MoO_4)_9$ and $(Y_{0,9}Eu_{0,1})_2O_3$ b) Absorption spectra of $(La_{0,9}Eu_{0,1})_2Zr_3(MoO_4)_9$ and $(Y_{0,9}Eu_{0,1})_2O_3$.

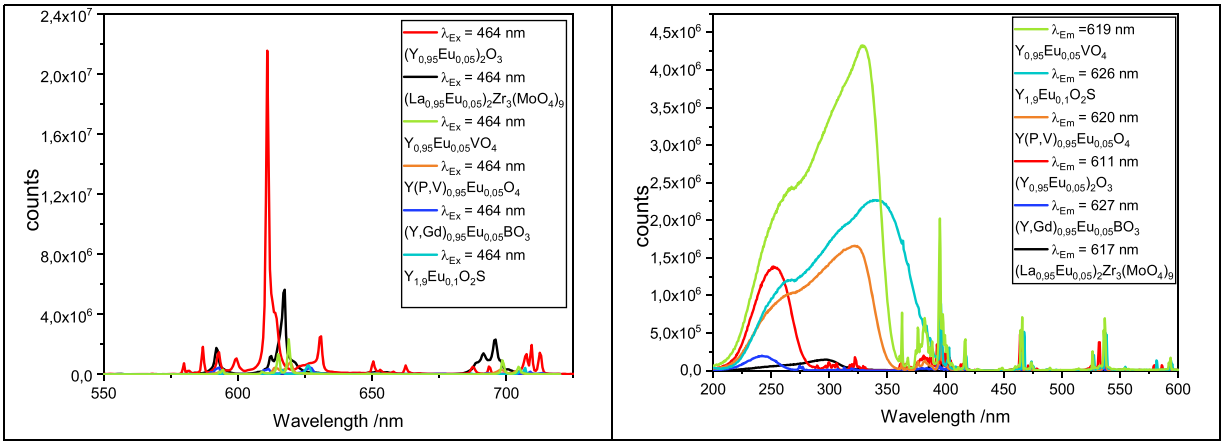

Fig. 6. a) Emission spectra of 5 % Eu^{3+} phosphors b) Corresponding excitation spectra of 5 % Eu^{3+} phosphors.

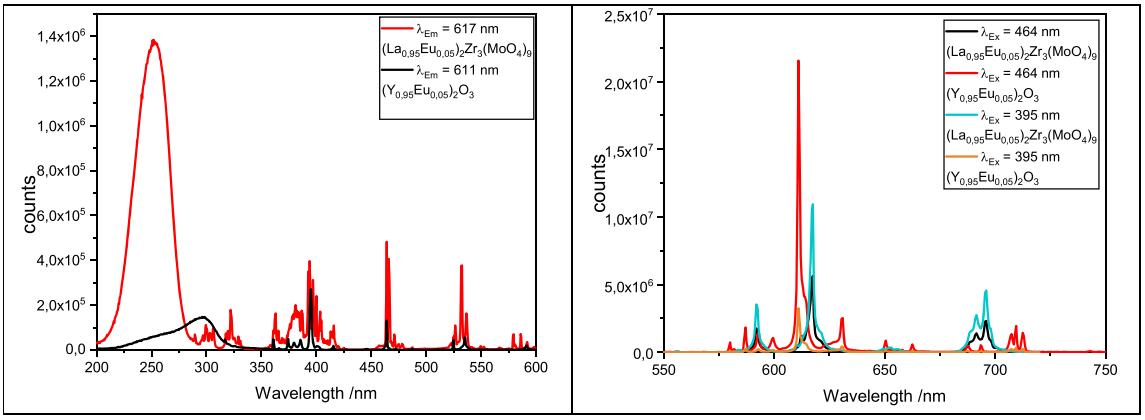

Fig. 7. a) Exciation spectra of 5 % Eu^{3+} $La_2Zr_3(MoO_4)_9$ and Y_2O_3 b) Corresponding Emission spectra of 5 % Eu^{3+} $La_2Zr_3(MoO_4)_9$ and Y_2O_3 at $\lambda_{Ex} = 464$ nm and $\lambda_{Ex} = 395$ nm.

with an Eu concentration of either 1 %, 5 %, or 10 % were prepared.

The XRD patterns of the prepared powders are depicted in Fig. 1. They confirm the presence of single-phase materials for all Eu^{3+} concentrations. The ionic radii of the isostructural materials differ only 7 % for La^{3+} and Eu^{3+} and only 5 % for Y^{3+} and Eu^{3+}. Hence, Vegard's law can be employed, as indicated by reference [9] and [34] consequently, a comprehensive series of solid solutions should be present, demonstrating a linear correlation of the host lattice parameter.

The reflection spectra depicted in Fig. 2a show the undoped $La_2Zr_3(MoO_4)_9$ (black line) and Y_2O_3 (red line). The band-to-band transitions can be described with the broad absorption that is observed for undoped $La_2Zr_3(MoO_4)_9$. The bottom of the conduction band most likely consists of empty 4d states of Zr^{4+} and Mo^{6+} or Y^{3+} and the top of the valence bands mainly of O^{2-} 2p states commonly in oxides. [9]

To calculate qualitative absorption spectra with the aid of the Kubelka-Munk function, the following formula was used. The scattering coefficient S can be estimated from the particle size of the powder [35].

$$S = \frac{1}{d_{50}}$$

$$A = \left(\frac{(1 - R(\lambda))^2}{2 * R(\lambda)}\right) * \frac{1}{d_{50}}$$

R = Reflectance value at λ; d_{50} = Mean particle size in cm; S = scattering coefficient in cm^{-1}

The obtained absorption spectra shown in Fig. 2b) indicates a strong difference between the two materials as the undoped $La_2Zr_3(MoO_4)_9$ is displaying a much higher absorption than the undoped Y_2O_3. The $La_2Zr_3(MoO_4)_9$ has an absorption strength of 660 cm^{-1} while the strength of Y_2O_3 is barely noticeable.

In Fig 3a) the reflection spectra of 1 % Eu^{3+} $La_2Zr_3(MoO_4)_9$ and Y_2O_3 is plotted. The reflection spectra of $La_2Zr_3(MoO_4)_9$ nearly looks the same as the one without Eu^{3+}. However, the Y_2O_3 has a noticeable red shift as an absorption is seen up to 350 nm slightly decreasing to 450 nm. In Fig 3b the changes in the reflection spectra can also be detected in the respective absorption spectra. Noticeable is the strong increase of the absorption strength. As the undoped material has its maximum at 660 cm^{-1} the material with 1 % Eu^{3+} at 1330 cm^{-1}.

Fig 4a) show the reflection spectra of 5 % Eu^{3+} $La_2Zr_3(MoO_4)_9$ and Y_2O_3. The typical Eu^{3+} lines can be observed. However, in $La_2Zr_3(MoO_4)_9$ the Eu^{3+} lines are much more prominent than in Y_2O_3. The high transition probability and strong absorption are linked to the band-to-band transitions which preserve the electron momentum. The observations can be transposed to Fig 4b). In the calculated absorption spectra the significant Eu^{3+} lines absorption lines can clearly be observed at 5 % Eu^{3+} $La_2Zr_3(MoO_4)_9$, whereas the 5 % Eu^{3+} doped Y_2O_3 depict solely very weak Eu^{3+}lines in the absorption spectra. The maximum of 5 % Eu^{3+} $La_2Zr_3(MoO_4)_9$ is around 1389 cm^{-1}. For comparison (Y,Gd)BO_3:Eu^{3+} and YVO_4:Eu^{3+} (Fig. 4c) as well as Y_2O_2S:Eu^{3+} and Y(P,V)O_4:Eu^{3+} (Fig. 4e) with an amount of 5 % Eu were measured under the same conditions as the other synthesized materials. As one can see, the calculated absorption of the reflectance spectra are significant lower than absorption of $La_2Zr_3(MoO_4)_9$ doped by 5 % Eu^{3+} but similar to 5 % Eu^{3+} comprising Y_2O_3 (Fig 4d, 4f). Additionally the charge transfer of the vanadate in comparison to the borate is observed in the reflection spectra in Fig. 4c. Y_2O_2S:Eu^{3+} and Y(P,V)O_4:$Eu^{3+}$are depicting relatively strong 4f-4f transitions and Urbach tailing, mainly originates from sulfur vacancies. A sulfur/oxygen to europium charge transfer can be observed in Y_2O_2S:Eu^{3+} and an oxygen to europium charge transfer in Y(P,V)O_4:Eu^{3+}.

Last but not least in Fig 5a) the reflection spectra of 10 % Eu^{3+} $La_2Zr_3(MoO_4)_9$ and Y_2O_3 are shown. Eu^{3+}lines are clearly visible in both spectra.

In Fig 5b) it is noticeable that even if the Eu^{3+} lines of the reflection spectra seem quite similar, $La_2Zr_3(MoO_4)_9$ has a much higher absorption strength than Y_2O_3. The main absorption at 466 nm has a difference of 134 cm^{-1} in $La_2Zr_3(MoO_4)_9$, while in the Y_2O_3 sample the difference is only 43 cm^{-1}. Even with the same Eu^{3+} concentration in the solid solution, the $La_2Zr_3(MoO_4)_9$ shows much higher absorbance than the equivalent Y_2O_3.

By taking a closer look at the emission spectra of the phosphors containing 5 % of Eu^{3+} at λ_{Ex} = 464 nm (Fig. 6a) it turns out that even though $La_2Zr_3(MoO_4)_9$:Eu^{3+} previously had shown much higher absorbance than the other Eu^{3+} phosphors, that isn't the case for the emission spectra. Y_2O_3:Eu^{3+} displays a much higher count rate than $La_2Zr_3(MoO_4)_9$:Eu^{3+} if excited at 464 nm, however $La_2Zr_3(MoO_4)_9$:Eu^{3+} indeed demonstrates a higher count rate than the other commercially used Eu^{3+} phosphors. Photoluminescence intensity is depending on the quantum yield and on the absorption strength! For commercially used phosphors, it can be assumed that the quantum yield is high in all materials. This indicates that the quantum yield of Y_2O_3:Eu^{3+} is higher than the quantum yield of $La_2Zr_3(MoO_4)_9$:Eu^{3+}.

By comparing the excitation spectra of 5 % $La_2Zr_3(MoO_4)_9$:Eu^{3+} and Y_2O_3:Eu^{3+} (Fig 7a) it is demonstrated that $La_2Zr_3(MoO_4)_9$:Eu^{3+} has its excitation maximum at 395 nm, not at 464 nm where the previous emission spectra were recorded. Y_2O_3:Eu^{3+}, however, show a better excitation at 464 nm. To compare the emission intensity, additional emission spectra upon 395 nm excitation were recorded. It can be noted that even if Y_2O_3:Eu^{3+} has still the highest emission from all measurements, $La_2Zr_3(MoO_4)_9$:Eu^{3+} has a higher emission intensity than Y_2O_3:Eu^{3+} at λ_{Ex} = 395 nm (Fig. 7b).

4. Conclusions

A comparison of several inorganic hosts for Eu^{3+} show significant differences in the absorption strength of the Eu^{3+} centered 4f-4f transitions. $La_2Zr_3(MoO_4)_9$ shows a significant higher absorption strength than other long known Eu^{3+} activated luminescent materials such as Y_2O_3:Eu, (Y,Gd)BO_3:Eu, Y_2O_2S:Eu, and YVO_4:Eu. A comparison of the emission and excitation spectra reveals that even though $La_2Zr_3(MoO_4)_9$ shows a significant higher absorption strength, the emission is still weaker than Y_2O_3 at 464 nm which can be explained with the assumed quantum yield of the materials. However, $La_2Zr_3(MoO_4)_9$ has indeed a higher emission intensity than Y_2O_3 at 395 nm excitation. This indicates that the material is advantageous for practical applications due to stronger photoluminescence and thus brighter emission for applications where an excitation of 395 nm is applied. With the use of $La_2Zr_3(MoO_4)_9$ less amount of Eu could be used in applications to achieve the same performance, resulting in a massive reduction in cost and economic benefits. However, in order to be able to assess whether $La_2Zr_3(MoO_4)_9$ would be a suitable phosphor e.g. for application in solid state lighting, further experiments are required with regard to the longevity of the product.

CRediT authorship contribution statement

Julia Exeler: Writing – original draft, Visualization, Project administration, Investigation. **Thomas Jüstel:** Supervision, Resources, Conceptualization.

Declaration of competing interest

The authors declare that they have no known competing financial interests or personal relationships that could have appeared to influence the work reported in this paper.

Data availability

Data will be made available on request.

Acknowledgements

The authors are grateful to the state of North Rhine Westphalia, Germany for financial support.

References

[1] W. Liu, R. Zuo;, Low temperature fired $Ln_2Zr_3(MoO_4)_9$ (Ln= Sm, Nd) microwave dielectric ceramics, Ceram. Int. 43 (2017) 17229–17232, https://doi.org/10.1016/j.ceramint.2017.09.083.

[2] S.G. Dorzhieva, Y.L. Tushinova, B.G. Bazarov, A.I. Nepomniashchikh, R. Y. Shendrik, Z.G. Bazarova;, Luminescence of Ln-Zr Molybdates; Bulletin of the Russian Academy of Sciences, Physics, 79 (2) (2015) 276–279, https://doi.org/10.3103/S1062873815020070.

[3] W. Liu, R. Zuo;, A novel low temperature firable $La_2Zr_3(MoO_4)_9$ microwave dielectric ceramic; J, Eur. Ceram. Soc., 38 (2018) 339–342, https://doi.org/10.1016/j.jeurceramsoc.2017.08.023.

[4] L. Shi, C. Liu, H. Zhang, R. Peng, G. Wang, X. Shi, X. Wang, W. Wang;, Crystal structure, Raman spectroscopy, metal compatibility and microwave dielectric properties of $Ce_2Zr_3(MoO_4)_9$ ceramics, Mater. Chem. Phys. 250 (2020) 122954, https://doi.org/10.1016/j.matchemphys.2020.122954.

[5] J. Zheng, C. Xing, Y. Yang, S. Li, H. Wu, Z. Wang;, Structure, infrared reflectivity spectra and microwave dielectric properties of a low-firing microwave dielectric ceramic $Pr_2Zr_3(MoO_4)_9$, J. Alloys Compd. 826 (2020) 153893, https://doi.org/10.1016/j.jallcom.2020.153893.

[6] X. Ma, C. Li, Z. Fa, H. Wu, Y. Zhang, Z. Zhang;, Crystal structure, Infrared spectra, and microwave dielectric properties of low-firing $Nd_2Zr_3(MoO_4)_9$ ceramics prepared by reaction-sintering process, J. Mater. Sci. Mater. Electron. 31 (2020) 12620–12627, https://doi.org/10.1007/s10854-020-03812-x.

[7] Y.H. Zhang, J.J. Sun, N. Dai, Z.C. Wu, C.H. Yang;, Crystal structure, infrared spectra and microwave dielectric properties of novel extra low-temperature fired $Eu_2Zr_3(MoO_4)_9$ ceramics, J. Eur. Ceram. Soc. 38 (4) (2019) 1127–1131, https://doi.org/10.1016/j.jeurceramsoc.2018.12.042.

[8] C.F. Xing, B. Wu, J. Bao, H.T. Wu, Y.Y. Zhou;, Crystal Structure, infrared spectra and microwave dielectric properties of a novel low-firing $Gd_2Zr_3(MoO_4)_9$ ceramic, Ceram. Int. 45 (17) (2019) 22207–22214, https://doi.org/10.1016/J.CERAMINT.2019.07.243.

[9] F. Baur, T. Jüstel;, New Red-Emitting Phosphor $La_2Zr_3(MoO_4)_9:Eu^{3+}$ and the Influence of Host Absorption on its Luminescence Efficiency; Aust, J. Chem., 68 (2015) 1727–1734, https://doi.org/10.1071/CH15268.

[10] J. Feng, W. Xie, X. Liu, X. Tang, L. Yan, H. Guo, A.A. Al Kheaif, H.S. Jang, J. Lin;, Multi-color luminescence evolution of $La_2Zr_3(MoO_4)_9:Ln^{3+}$ (Ln^{3+}= Dy^{3+} and/or Eu^{3+}) nanocrystalline phosphors for UV-pumped white light emitting devices; J, Lumin., 203 (2018) 179–188, https://doi.org/10.1016/j.jlumin.2018.06.032.

[11] G.A. Hirata, J. McKittrick, M. Avalos-Borja, J.M. Siqueiros, D. Develin;, Physical properties of Y_2O_3:Eu luminescent films grown by MOCVD and laser ablation; Appl, Surf. Sci. 113/114 (1997) 509–514, https://doi.org/10.1016/S0169-4332(96)00829-X.

[12] J. Dhanaraj, R. Jagannathan, T.R.N. Kutty, L. Chung-Hsin;, Photoluminescence Characteristics of $Y_2O_3:Eu^{3+}$ Nanophosphors Prepared Using Sol-Gel Thermolysis; J, Phys. Chem. B, 105 (45) (2001) 11098–11105, https://doi.org/10.1021/jp0119330.

[13] L.E. Shea, J. McKittrick, O.A. Lopez, E. Sluzky;, Synthesis of Red-Emitting, Small Particle Size Luminescent Oxides Using an Optimized Combustion Process, J. Am. Ceram. Soc. 9 (12) (1996) 3257–3265, https://doi.org/10.1111/j.1151-2916.1996.tb08103.x.

[14] X. Yong-Nian, G. Zhong-Quan, W.Y. Ching;, Electronic, structural, and optical properties of crystalline yttria, Phys. Rev. 56 (23) (1997) 14993–15000, https://doi.org/10.1103/PhysRevB.56.14993.

[15] W.H. Yen, S. Shionoya, H. Yamamoto;, Phosphor Handbook, CRC Press, 2006. ISBN: 0-8493-3564-7.

[16] W. Chen, M. Zhuo, Y. Liu, S. Fu, Y. Liu, Y. Wang, Z. Li, Y. Li, Y. Li, L. Yu, Uniform octahedral-shaped $Y_2O_3:Eu^{3+}$ submicron single crystals: Solid-state synthesis, formation mechanism and photoluminescence property, J. Alloys Compd. 656 (2016) 764–770, https://doi.org/10.1016/j.jallcom.2015.10.047.

[17] S. Som, S. Das, S. Dutta, H.G. Visser, M.K. Pandey, P. Kumar, R.K. Dubey, S. K. Sharma, Synthesis of strong red emitting $Y_2O_3:Eu^{3+}$ phosphor by potential chemical routes: comparative investigations on the structural evolutions, photometric properties and Judd-Ofelt analysis, RSC. Adv. 5 (87) (2015) 70887–70898, https://doi.org/10.1039/C5RA13247A.

[18] S. Gai, C. Li, P. Yang, J. Lin, Recent progress in rare earth micro/nanocrystals: soft chemical synthesis, luminescent properties, and biomedical applications, Chem. Rev. 114 (4) (2014) 2343–2389, https://doi.org/10.1021/cr4001594.

[19] D.K. Williams, B. Bihari, B.M. Tissue, Preparation and fluorescence spectroscopy of bulk monoclinic $Eu^{3+}:Y_2O_3$ Nanocrystals, J. Phys. Chem. 102 (1998) 916–920, https://doi.org/10.1021/jp972996e.

[20] W. Wang, P. Zhu, Red photoluminescent Eu^{3+}-doped Y_2O_3 nanospheres for LED-phosphor applications: Synthesis and characterization, Opt. Express 26 (2018) 34820–34829, https://doi.org/10.1364/OE.26.034820.

[21] J. Geusebroek, R. Boomgaard, A. Smeulders, H. Geerts, Color invariance, IEEe Trans. Pattern. Anal. Mach. Intell. 23 (12) (2001) 1338–1350, https://doi.org/10.1109/34.977559.

[22] D. Ebert, Articular cartilage optical properties in the spectral range 300–850 nm, J. Biomed. Opt. 3 (3) (1998) 326, https://doi.org/10.1117/1.429893.

[23] L. Yang, S. Miklavcic, Revised kubelka–munk theory iii a general theory of light propagation in scattering and absorptive media, Journal of the Optical Society of America A 22 (9) (2005) 1866, https://doi.org/10.1364/josaa.22.001866.

[24] P. Mudgett, L. Richards, Multiple scattering calculations for technology, Appl. Opt. 10 (7) (1971) 1485, https://doi.org/10.1364/ao.10.001485.

[25] A. Roy, R. Ramasubramaniam, H. Gaonkar, Empirical relationship between kubelka–munk and radiative transfer coefficients for extracting optical parameters of tissues in diffusive and nondiffusive regimes, J. Biomed. Opt. 17 (11) (2012) 115006, https://doi.org/10.1117/1.jbo.17.11.115006.

[26] L.E. McNeil, R.H. French, Light scattering from red pigment particles: multiple scattering in a strongly absorbing system, J. Appl. Phys. 89 (1) (2001) 283–293, https://doi.org/10.1063/1.1331344.

[27] P. Kubelka, F. Munk;, An article on optics of paint layers, Z. Tech. Phys. 12 (1931) 593–601. http://www.graphics.cornell.edu/~westin/pubs/kubelka.pdf.

[28] G. Meichsner, J. Schröder;, Lackeigenschaften messen und steuern, Vincentz Network GmBH (2003). ISBN: 3-86630-634-2.

[29] A.I.S. Silva, N.B.D. Lima, A.M. Simas, S.M.C. Gocalves, Europium Complexes: Luminescence Boost by a Single Efficient Antenna Ligand, ACS. Omega 2 (2017) 6786–6794, https://doi.org/10.1021/acsomega.7b00647.

[30] B. Alpha, R. Ballardini, V. Balzani, J.M. Lehn, S. Perathoner, N. Sabbatini;, Antenna Effect in Luminescent Lanthanide Cryptates: A Photophysical Study, Photochem. Photobiol. 52 (1990) 299–306, https://doi.org/10.1111/j.1751-1097.1990.tb04185.x.

[31] G. Vicentini, L.B. Zinner, J. Zukerman-Schpector, K. Zinner;, Luminescence and Structure of europium compounds, Coord. Chem. Rev. 196 (2000) 353–382, https://doi.org/10.1016/S0010-8545(99)00220-9.

[32] IUPAC, Compendium of Chemical Terminology (1997). ISBN: 0865426848.

[33] R. Serway, C. Moses, C. Moyer; Modern Physics; Brooks/Cole (2004); ISBN: 0534493394.

[34] L. Vegard;, Die Konstitution der Mischkristalle und die Raumfüllung der Atome, Z. Phys. 5 (1921) 17–26, https://doi.org/10.1007/BF01349680.

[35] G. Kortüm, D. Oelkrug, Über den Streukoeffizienten der Kubelka-Munk-Theorie, Zeitschrift für Naturforschung A 19 (1964) 28–37, https://doi.org/10.1515/zna-1964-0107.